Single Reflection Spatial Voting: A Novel Method for Discovering Reflective Surfaces Using Indoor Positioning Systems

R. K. Harle
Laboratory for Communication Engineering, University of Cambridge, UK
rkh23@cam.ac.uk

A. Ward
Ubiquitous Systems Limited
andy.ward@ubiquitous-systems.com

A. Hopper
Laboratory for Communication Engineering, University of Cambridge, UK
hopper@eng.cam.ac.uk

Abstract

We present a novel method of using reflected pulses in indoor ultrasonic positioning systems to infer the details of reflective objects in the environment. The method is termed Single Reflection Spatial Voting (SRSV), and we perceive its major use to be in the field of pervasive computing, where automated object and surface discovery is emerging as an important feature.

We demonstrate use of the method in the case of searching for vertical walls using an existing ultrasonic position sensor system (the Bat system). We find that valuable information can be extracted from reflection data using SRSV, and are able to construct a model of the room using a simple algorithm. We conclude that this method can be used to extract base data upon which to build hypotheses about the environment, given further sensor analysis.

We also briefly address the potential uses of SRSV in Ultra-Wideband positioning, autonomous navigation, and map building.

1 Introduction

Much of the current research in location systems concentrates on creating an accurate and reliable indoor positioning system, the perceived use of which is as a major component of a pervasive, context-aware computing system. Indoor positioning systems typically rely on the propagation of a physical wave phenomenon, such as ultrasonic or radio waves. The prevalence of reflecting surfaces in indoor environments drastically reduces the accuracy and reliability of positions returned from such systems. We present a method to turn this apparent weakness into a potential strength. We use reflected signals to help automate the process of modelling the environment within which the sensor network is operating.

Our experiences with a context-aware system [1] tell us that useful and reliable applications stem from having both an accurate position for an object or person, *and* from knowing details about the environment within which they are positioned. Presently, such environmental information is painstakingly entered by hand (for example, wall vertices, table positions, workstation locations) to allow a meaningful virtual model of the world to be formed (see Figure 1).

Once a useful model is established, it must also cope with the inherent dynamic nature of human environments. The applicability of a model diminishes rapidly as it loses synchronisation with the world. To remain useful, context-aware systems must be able to adapt to changing environments. Our experiences suggest that such adaptation can only stem from the coordination of sensor systems and processing methods. In this paper, we present a powerful method based on the principle that important environment information is superimposed on the positioning signals, in particular the reflections.

Given details of reflecting surfaces, we can de-

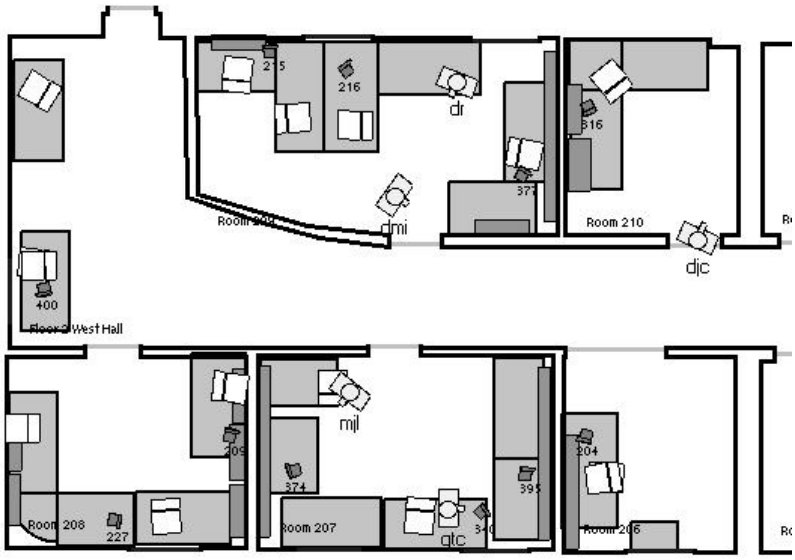

Figure 1: A screen shot from a real-time environment monitoring application in daily use.

velop better models of the world, allow for dynamic reconfiguration of the environment, and potentially provide feedback into a positioning system to improve accuracy. We stress that, whilst we present much of the paper in the context of an ultrasonic positioning system (the Bat system), the general method has potential uses outside of ultrasonic systems.

The essential requirement of the method is that the positioning medium interacts with objects within the environment, giving rise to reflected signals. Standard media used in positioning systems to date (ultrasound [16, 12, 14], radio [2, 3]) all suffer from environmental reflections, and this has traditionally been a large source of error. In addition, technologies expected to offer ubiquitous positioning in the future, such as Ultra Wideband radio, are susceptible to reflections.

2 The Bat Ultrasonic Location System

The Bat system is a real-time positioning system for people and objects in an indoor environment [16]. The system has previously been implemented as a major component of a context-aware, pervasive computing system [1]. One installation of the Bat system covers the upper floor of the Laboratory for Communication Engineering, encompassing an area of approximately 550m^2, and provides a true context-aware computing environment in daily use.

As described in [1], the Bat system is based around wireless active tags (“Bats”) worn by users or attached to objects. A radio signal from a central controller triggers each Bat in turn, at a known time. When triggered, each Bat emits an ultrasonic pulse, which is received by a matrix of receivers placed at accurately known locations in the ceiling. By measuring the time delays between emission and reception of pulses, we gain estimates of the distance travelled by the pulse to each receiver within range. We then use a multilateration algorithm to convert the distance measurements to a location for the Bat in three-dimensional space [10].

2.1 Identifying Reflections Through Multilateration Algorithms

The Bat system operates in indoor office-like environments, which contain many objects and surfaces that specularly reflect ultrasound (such as computer monitors and walls). The pulse emitted by a Bat may travel directly to a receiver (a

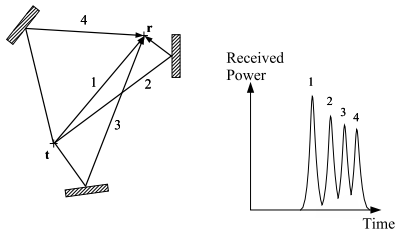

(a) Three obstructions give rise to a direct-path signal peak (1) and three multipathed peaks (2,3,4) in the power profile of the received signal

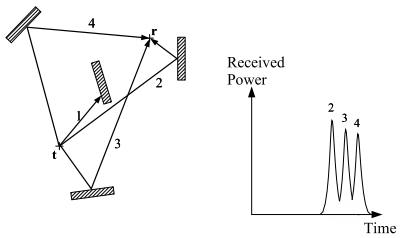

(b) A further obstruction hinders the direct-path signal

Figure 2: Illustration of multipathed signal propagation between a receiver, r, and a transmitter, t

direct-path signal), but may also arrive after a reflection from one or more objects or surfaces in the environment (a multipathed signal). Multipathed signals do not provide information about the true (direct-path) distance of the Bat from the receiver, and hence it is important to identify and eliminate them from further processing.

In situations where a direct-path signal reaches a receiver, the Bat system can be sure that any subsequent pulse arrivals correspond to multipathed signals, because any reflected paths must necessarily be longer than the direct-path (Figure 2(a)). However, it is not always the case that the direct-path signal reaches the receiver, and in these situations the first signal to arrive at the receiver will, in fact, be a multipathed signal (Figure 2(b)). The positioning algorithm used in the Bat system is therefore designed to identify and reject multipathed signals, and we present here a simplified overview of that algorithm and the heuristics it uses (further details are available in [16]).

Following the emission of a pulse by a Bat, and its subsequent reception, we have a series of time-of-flight measurements. We convert these time measurements to distances using the well-documented temperature variation of the speed of sound [6]. We wish to derive four quantities from this information; the components of the Bat location (x,y,z), and an estimate of the positioning standard error. To do so, then, we require a minimum of four (non-multipathed) readings.

The process of identifying and excluding multipathed signals begins by forming a nonlinear model [13] of all the data, providing an estimate of the four quantities we are interested in. The error estimate is used to evaluate the model fit. If it exceeds the known accuracy of the system (approximately 3cm), we evaluate the residuals for each distance measure and order them numerically. Traditional nonlinear model algorithms order the magnitude of these residuals and discard the data associated with the largest and reprocess, thereby removing the outliers and improving the result. We use a different approach to capture the physical principle that no signal may arrive at a receiver early (corresponding to movement faster than the speed of sound), but only late (corresponding to a multipathed measure).

If we define $d_{measured}$ as the measured distance from a Bat to a particular receiver, d_{model} as the distance calculated by the model for the same quantity, then we can define the residual, e, as being directly proportional to

$$e \propto (d_{measured} - d_{model}) \qquad (1)$$

If we assume that the model has converged spatially close to the correct position, this quantity is negative when the model requires the signal to exceed the speed of sound, and positive when the signal appears to be multipathed (relative to the model predictions). We can adopt this as a general heuristic, since it fails only in the unlikely case of the majority of received signals being multipathed due to a specular object, causing the model to converge on a reflection image.

Since the speed of sound is fixed, but multipathed signals are likely, we maintain the sign of the residual, and discard the largest positive residual as multipathed. We repeat the process of modelling and discarding the measurement associated with the largest positive residual until

we reach the required accuracy level, or until there are less than four measures remaining (a failure). Consequently, when we return a position, we have classified the initial distance measures into two groups; consistent with the position (assumed non-multipathed), and inconsistent (assumed multipathed). The Bat system receivers are also capable of recording the time-of-arrival of any *second* pulse they receive (which corresponds, as described earlier, to a multipathed signal). With each position, then, we can identify multipathed signals by:

1. Rejection from the positioning algorithm as described above.

2. Reception of a second pulse at a receiver that returned a first pulse consistent with the position calculated.

Whereas the Bat system rejects this reflection information as being of no use in computing location information, we now turn our attention to a method of using this data to derive information about the environment.

3 Single Reflection Spatial Voting (SRSV)

Barshan has described a spatial voting scheme for determining *two dimensional* surface profiles using ultrasonic rangefinders mounted on a mobile robot [5, 4]. The method associates a circular arc centred on the known position of the ultrasonic transceiver for each range measure, with a radius equal to half the distance covered by the ultrasonic pulse. By collecting a series of results from sufficiently different transceiver positions (generated by a number of rangefinders on the robot and/or by moving the robot platform), we expect to observe the highest density of arc intersections along the locus of the surface, as illustrated in Figure 3. Spatial voting splits the two dimensional plane into a regular grid of cells. With each cell, we associate a number representing the number of arcs which intersect its bounds. We can then extract a representation of the surface, quantised to the cell size, by searching the grid for high densities of intersections.

We present here a novel and significant extension to Barshan's method which uses a *three dimensional* Single Reflection Spatial Voting (SRSV) grid. This approach differs from that of

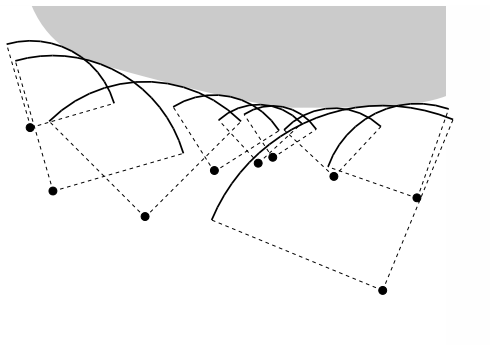

Figure 3: An illustration of the two dimensional surface extraction based on rangefinders (shown as black circles). The grey area represents the surface of interest, and the arc of each circle segment corresponds to the range reading from a specific rangefinder.

Barshan, since we use a physically distinct ultrasonic transmitter and receiver, an infrastructure that is in place and static, and a series of only multipathed measurements. SRSV is particularly suited to the pervasive computing environment because it allows incremental updating as more reflections are captured, but does not require that the details for each reflection be individually stored, thereby reducing storage requirements. We make the assumption that multipathed pulses have reflected only once; we have demonstrated that the method is sufficiently robust that multiple reflections do not render the method invalid in practice. In three dimensions, with a separate receiver and transmitter, the two dimensional circular arcs described by Barshan become prolate spheroids with foci at each of the receiver and transmitter locations, and the SRSV grid segments the volume into regular cubes ("cells"). Analysis of the density of spheroid intersections in each cell provides data about the environment, such as the locations of walls and specular objects.

3.1 The Prolate Spheroid of Reflection

Consider two points in three dimensional space representing a transmitter, $\mathbf{t}$, and a receiver, $\mathbf{r}$, and a signal that propagates between them via a single specular reflection from a point on a surface, $\mathbf{P}$. If the distance travelled by the signal is known (through time-of-flight measurement for example), the allowed locus of the reflection point is a prolate spheroid with major axis b and

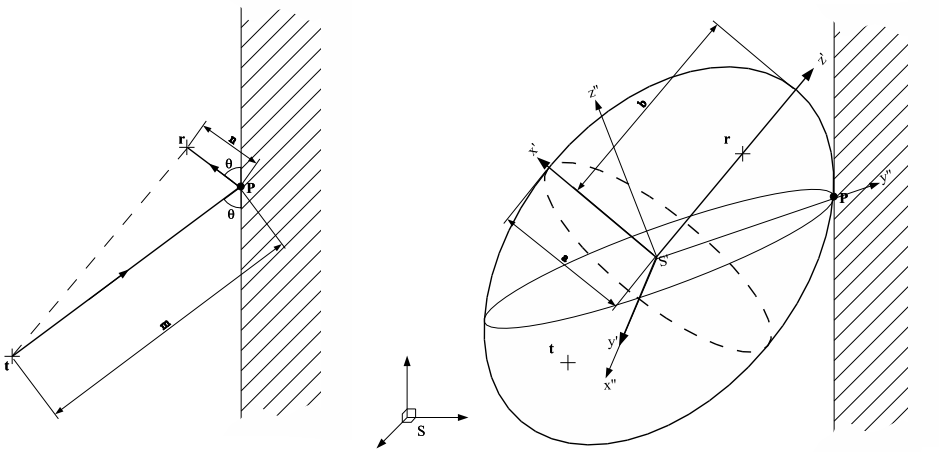

Figure 4: The reflection geometry for a single reflection from a point $\mathbf{P}$ between a transmitter at $\mathbf{t}$ and a receiver at $\mathbf{r}$, with a multipathed length of $l = m + n$. The thick outline (right) shows the associated prolate spheroid, and the thin outline shows the elliptical locus of $\mathbf{P}$ if we assert that it is on a *vertical* wall.

minor axis a (the shape formed by rotation of a two dimensional ellipse about its major axis), as shown in thick outline in Figure 4. Such a surface can be described in its principal co-ordinate frame (marked S' in Figure 4) by the matrix formulation,

$$\mathbf{x}'^{\mathrm{T}}\mathbf{A}'\mathbf{x}' = 1 \tag{2}$$

where $\mathbf{x}'$ represents a general three dimensional vector in S', and the matrix $\mathbf{A}'$ has components,

$$\mathbf{A}' = \begin{pmatrix} \frac{1}{a^2} & 0 & 0 \\ 0 & \frac{1}{a^2} & 0 \\ 0 & 0 & \frac{1}{b^2} \end{pmatrix} \tag{3}$$

where a and b are are the major and minor axes as shown in Figure 4. We derive these quantities from the path length travelled by the reflected pulse, l, as defined in Figure 4. Using simple geometrical arguments, we find:

$$\begin{aligned} a &= \frac{1}{2}\sqrt{l^2 - |\mathbf{t} - \mathbf{r}|^2} \\ b &= \frac{l}{2} \end{aligned} \tag{4}$$

To describe this in co-ordinate frame S, our 'real world' frame, we apply a translation to make the origins coincident, and use Rodrigues' rotation formula [11] to calculate the relevant rotation matrix, $\mathbf{R}$, such that

$$\mathbf{x}' = \mathbf{R}(\mathbf{x} - (\mathbf{t} + \frac{1}{2}(\mathbf{r} - \mathbf{t}))) = \mathbf{R}(\mathbf{x} - \mathbf{u}) \tag{5}$$

By transforming a regular three dimensional grid in system S to S' we can use geometry to calculate the intersection of this prolate spheroid with the cells, forming an SRSV grid for arbitrary surfaces. However, in pervasive systems we are usually able to restrict our interest to a subset of surfaces such as vertical walls, near-vertical screens, horizontal tables, etc. Such restrictions allow refinement of the method. As an example, in this paper we will be primarily interested in vertical surfaces, for which we wish to restrict the locus of $\mathbf{P}$ to spheroid points with a normal lying in the horizontal plane of S. To see this, consider the function,

$$f(\mathbf{x}) = |\mathbf{x} - \mathbf{t}| + |\mathbf{x} - \mathbf{r}| \tag{6}$$

which represents the path length for $\mathbf{t}$ to $\mathbf{x}$ to $\mathbf{r}$. The quantity $\nabla f(\mathbf{x})$ will point in the direction of the sum of the unit vectors of $(\mathbf{t} - \mathbf{x})$ and $(\mathbf{r} - \mathbf{x})$, which bisects the angle between these two vectors. Thus, $\nabla f(\mathbf{x})$ points in the direction of the normal to the reflecting surface for a specular reflection from $\mathbf{t}$ to $\mathbf{r}$. The spheroid is defined by the relation

$$f(\mathbf{x}) = l \tag{7}$$

and hence $\nabla f(\mathbf{x})$ points in the direction of the normal to the spheroid at $\mathbf{x}$. i.e. The tangent plane at any point on the spheroid is the reflecting surface that reflects a signal from $\mathbf{t}$ to $\mathbf{r}$, and by symmetry the locus of $\mathbf{P}$ is then the intersection of the spheroid with a plane which passes through the origin of S'.

To describe this intersection, we define a further co-ordinate system, S'', which has the same origin as S', but with the $\mathbf{z}''$ direction normal to the intersection plane, and the $\mathbf{y}''$ direction perpendicular to this, but within the vertical plane containing both $\mathbf{r}$ and $\mathbf{t}$ (see Figure 4). We can link the frames S' and S'' by a rotation matrix, $\mathbf{R}'$, such that

$$\mathbf{x}'' = \mathbf{R}'\mathbf{x}' \tag{8}$$

To set up the axes in practice, we calculate a point of intersection ($\mathbf{P}$ in Figure 4) of the vertical plane through $\mathbf{r}$ and $\mathbf{t}$ with the spheroid, and with a horizontal normal. Then we calculate a point on the spheroid with $z' = 0$ and a horizontal normal. Combined with the S' origin, we then have three non-co-linear points; sufficient to derive the plane normal, $\mathbf{n}'$. When $\mathbf{n}'$ is normalised, (8) implies that

$$\mathbf{R}'\mathbf{n}' = \begin{pmatrix} 0 \\ 0 \\ 1 \end{pmatrix} \tag{9}$$

We choose y'' to point from the origin to the point $\mathbf{P}$, which implicitly defines the direction of $\mathbf{x}'$ in the Cartesian S' frame. We can then relate the frames S' and S'' by a rotation matrix $\mathbf{R}'$ and assert,

$$\mathbf{x}''^{\mathrm{T}}\mathbf{R}'\mathbf{A}'\mathbf{R}'^{\mathrm{T}}\mathbf{x}'' = \mathbf{x}''^{\mathrm{T}}\mathbf{A}''\mathbf{x}'' = 1 \tag{10}$$

which, referring back to (2), defines an elliptical intersection in the $z'' = 0$ plane.

Once the ellipse parameters have been calculated, we can perform SRSV by transforming the vertices of SRSV cells to that co-ordinate system, and searching for interceptions of the faces with the ellipse.

3.2 Using The Spheroid Normals

We can extend the basic premise of SRSV by accounting for surface normals, vastly simplifying any subsequent analysis. When a spheroid intersects a cell, there is an associated average normal to the spheroid within that cell. If there is to be a reflecting surface giving rise to that spheroid within that cell, it must have a normal direction parallel to the spheroid normal. Thus, we can associate each SRSV vote within a cell with a particular three dimensional normal direction. In practice, we associate a series of angular bins with each cell, and add votes to the angular bin that contains the average spheroid normal within that cell. If a planar reflecting surface exists within that cell, the SRSV count for the angular bin containing its normal direction should vastly exceed the counts in the remaining angular bins.

When considering vertical walls, we need only associate cells with angular bins in the horizontal plane. We calculate the average normal to the ellipse within each cell it intersects, project that direction into the horizontal plane and increment the relevant angular bin for the cell. This is a particularly useful representation when searching for walls, since we are really searching for contiguous, vertical, planar surfaces that extend across multiple cells, all with high SRSV counts in the angular bin corresponding to the surface normal.

4 Implementation and Results

Experimental validation was performed by post-processing real reflections collected from the Bat system. We have logged the reflections, caught in a communal coffee area, for Bats worn by personnel for a period of two days, producing a distribution of sightings and reflections typical for an area in daily use. Figure 5 illustrates the shape of the area and any fixed objects (hatched) and identifies three key Regions within it (labelled 1,2,3). Region 1 is used as a through-way, with people rarely stopping. Consequently, we see a low number of sightings here. Region 2 is a general communal area, where people tend to congregate and remain for extended periods of time, building up large numbers of sightings. Region 3 is an area with a low density of Bat receivers in the ceiling, and a high density of ceiling obstructions. Relative to Regions 1 and 2, sightings are rare here.

Figure 5(b) shows the actual distribution of sightings collected during the test period. This data was processed using an SRSV cell size of 0.2m, using 6897 collected reflections. The initial result is shown in Figure 6; the SRSV counts shown are the sums of each vertical column of SRSV cells. This ‘collapsed column’ representation helps to capture the fact that the walls are vertical and thus all cells in a vertical column provide evidence for a wall at that position. The highly non-uniform usage of the area by personnel is reflected in the results. We see a high density of intersections in Region 2, a direct result of users remaining in roughly the same place for many sightings, building up intersections in that

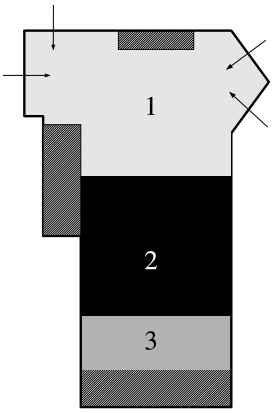

(a) A schematic view of the communal coffee area

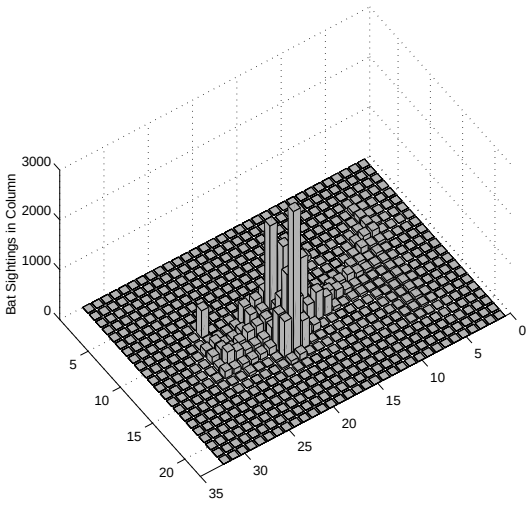

(b) The distribution of sightings collected during testing

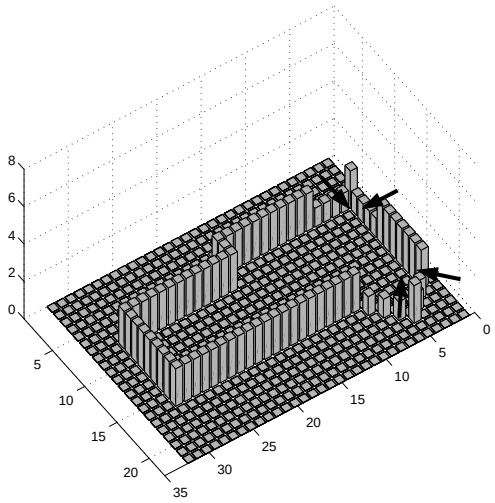

(c) A representation of the room walls using the same collapsed column grid as (b). The arrows show door positions.

Figure 5: The testing area

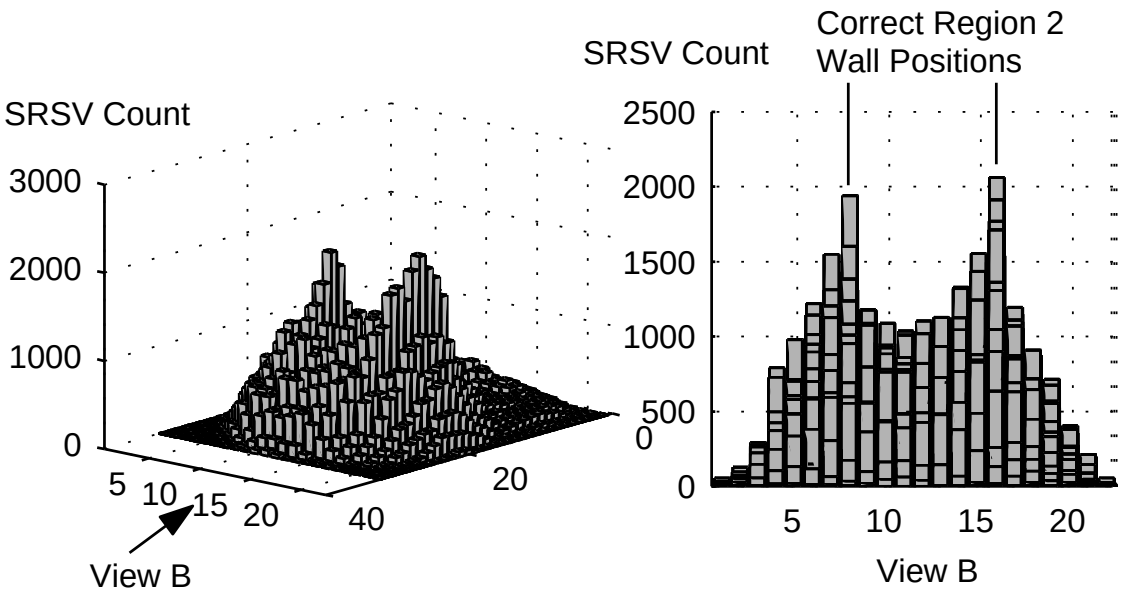

Figure 6: The column-collapsed SRSV grid for the coffee area from a series of viewing angles

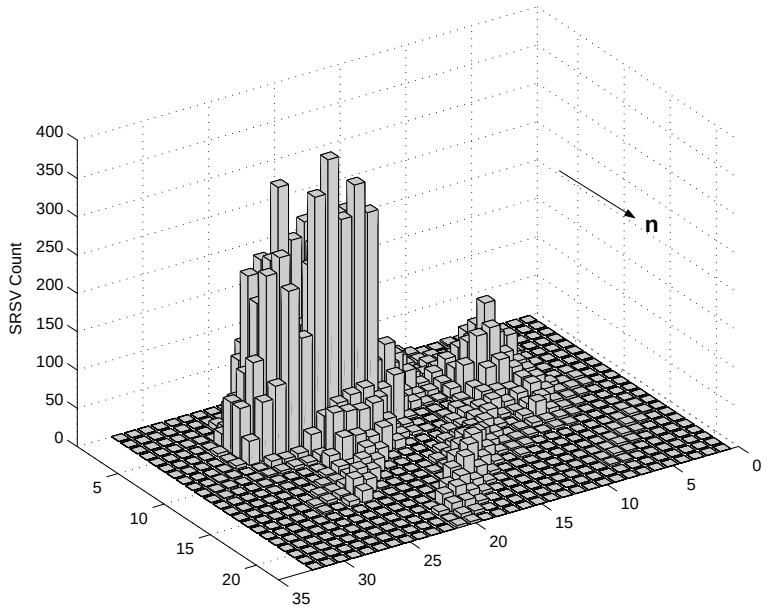

Figure 7: The SRSV count for angular bins containing direction $\mathbf{n} \pm 10°$.

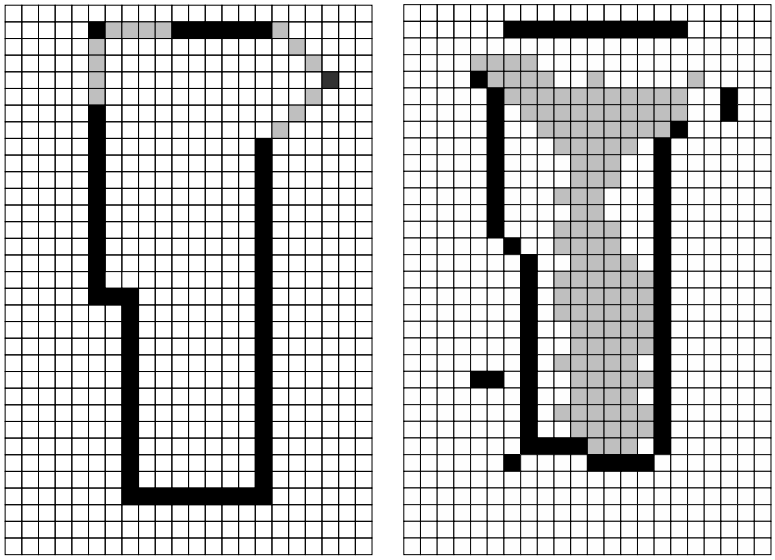

(a) Correct representation of the test area (grey cells represent doors).

(b) Results of SRSV (grey cells show the eroded sighting distribution)

Figure 8: SRSV Results

Region. There are strong maxima in the SRSV counts in Region 2, which correctly trace out the walls on either side. Note that the SRSV count inside this Region is non-zero, increasing with the number of sightings, despite the fact that there can be no wall there. This potentially misleading situation illustrates the need to store the SRSV normal directions in angular bins. Figure 7 shows the same data, but for a specific angular bin of width 20° containing the wall normal direction. We see that the SRSV counts within Region 2 are drastically reduced, since the high counts in Figure 6 are distributed across the angular bins in the SRSV cell.

We can further improve each angular view by excluding cells in a column that has seen a sighting of a Bat (thereby implying no wall can be there). In practice, to account for positioning inaccuracies and the small possibility of a wall and a Bat coexisting within a cell of finite size, we have found it best to erode the area of sightings by one cell in every direction. This leaves us with a core shape of sightings that we are confident covers cells that do not contain walls. To encapsulate this fact, we zero the SRSV count for any column within which a Bat was sighted.

To extract the wall positions, we applied the following simple algorithm for the four normal directions that follow the axes of the SRSV grid:

1. Create the SRSV grid for the angular bin containing the normal (e.g. Figure 7) of interest.
2. Set SRSV counts to zero for cells contained in the eroded region of sightings
3. Scan the grid perpendicular to the normal direction, amalgamating cells with non-zero SRSV counts into single 'walls', allowing a maximum gap of two cells (0.4m) within each. This gap allows for wall continuity across regions of low or no occupancy.
4. Calculate the average SRSV count for each wall, and assign the value to each cell within the wall.
5. Scan the grid parallel to the normal direction, taking the cell with the maximum average SRSV count as containing a wall.

The results of applying this algorithm are presented in Figure 8, and are encouraging.

The position and orientation of the longer side walls has been correctly extracted, with the overall room shape being determined to a good approximation. Despite the vastly different uses of

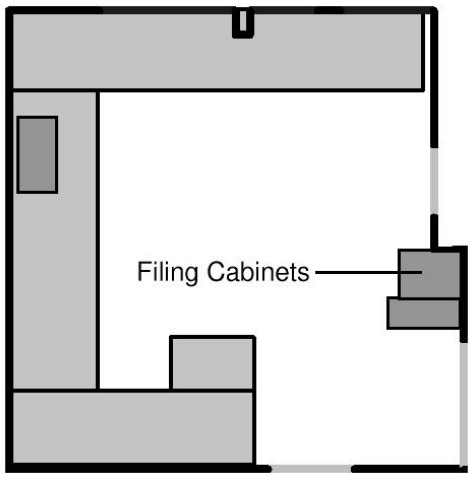

(a) A graphical representation of the room and its furniture

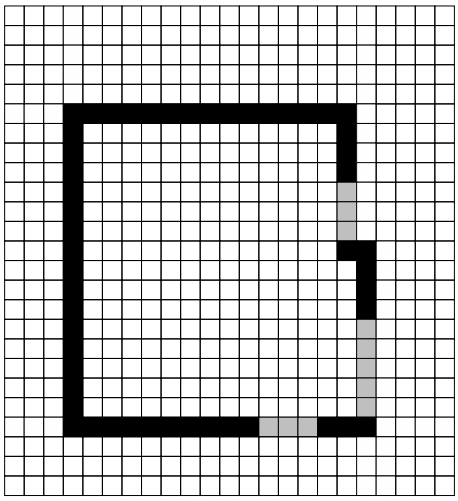

(b) Correct Representation of the room on the SRSV grid

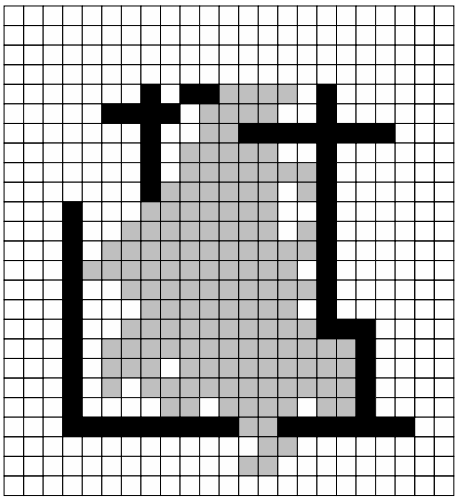

(c) Results of SRSV (grey cells show eroded sighting distribution)

Figure 9: The results of applying SRSV to another room.

Regions 1 and 2, we are still able to extract the wall positions with good accuracy. The door positions, shown in Figure 8(a), are clearly present, with the exception of the top-most door. This door leads to an office that was not in use during testing, and hence the door remained closed, completing the wall.

Importantly, the method is clearly superior to simply using the sighting distribution to determine the room shape, as shown by the shaded region of Figure 8(b). The SRSV method is capable of inferring wall positions in areas penetrated by ultrasonic signals, but where Bats are not sighted. This is a useful feature in office environments, where desks and machines typically obstruct users from entering areas adjacent to walls.

The extraction algorithm used works well when we specify the normal axes to examine. However, the vast majority of office buildings contain rectangular rooms, so such a scenario is not contrived. The principal axes may be entered by hand, or we may make the assumption that once the orientation of one room or wall is determined, we give precedence to the same normal direction (and those parallel and perpendicular to it) throughout the building. Determination of a single wall orientation is possible by simply looking for a long sequence of cells with locally high SRSV counts in angular bins consistent with the sequence normal, or by using more complex image techniques such as a Hough Transform [8].

For comparison, Figure 9 gives a representation of another room within our Laboratory, and the results of applying SRSV analysis to sightings recorded within it over a period of three days. Here, we find the results to be similarly encouraging. The absence of a colleague who sits in the top left corner of 9(a) during the testing period resulted in poor determination of walls in that area, as expected. However, the remaining wall positions were correctly determined. In particular, it is interesting to note that the filing cabinets marked in 9(a) were treated as an extension of the wall nearby due to the large, smooth and vertical surface they presented.

5 Data Evolution

To demonstrate the evolution of SRSV data as sightings are collected, a further dataset was collected from within a long, straight corridor. This gave a further opportunity to test the method, and a very strong feature to examine, in the form of one of the walls.

A total of 4000 sightings were analysed, collected over a period of one day. Figure 10 shows a series of views of the collapsed grid count for a normal direction perpendicular to one of the walls after different numbers of sightings, n. The correct wall position lies within the bin labelled 10 in the graphs. The evolution of a peak within this bin is clearly evident.

It is important to realise that we cannot accurately define the number of sightings required to extract a feature. There is no guaranteed number of single reflections associated with each sighting, and furthermore no guarantee that the sightings are distributed in such a way as to produce reflections along the entire length of the feature. This can be observed in Figure 10 by the apparent lack in difference between 10(f) and 10(g). Nevertheless, the graphs shown in Figure 10 serve to illustrate a typical evolution.

6 Further Applications of SRSV

SRSV offers the opportunity to detect static and dynamic details of great use to the pervasive computing community. Whilst in this paper we have applied SRSV analysis in the context of static vertical walls, the concept is not limited to them. We can also detect other vertical features, such as dynamic walls (temporary partitions), door positions and states (open or closed), and positions and orientations of monitors (particularly useful in the context of hot-desking).

Note that the analysis algorithm for the SRSV grid may need to be tailored to extract features of limited extent, such as monitors. The algorithm presented above searches for long, contiguous lines within the collapsed grid, which we would not expect to observe for monitors. Instead, we would search for well-defined, bounded planes of normals at heights useful for displays.

It is possible to apply the same ideas to non-vertical surfaces by a straightforward coordinate rotation. In the specific case of the Bat system, however, there is little information to be gained about non-vertical surfaces. This is due to the directional nature of the ultrasonic emission from a Bat.

Since the Bat receivers are designed to be ceiling mounted, the ultrasonic emission from Bats is designed to be directed primarily upward, toward the ceiling. Furthermore, for most of time Bats

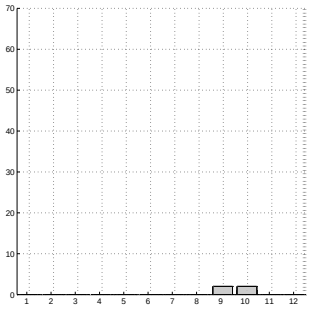

(a) n=10

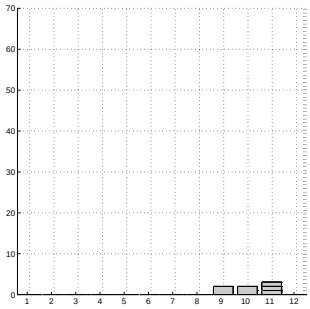

(b) n=100

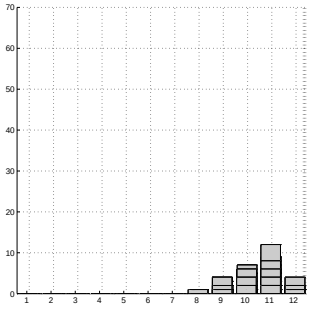

(c) n=500

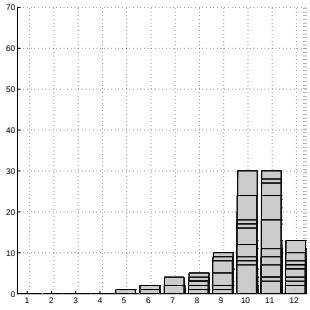

(d) n=1000

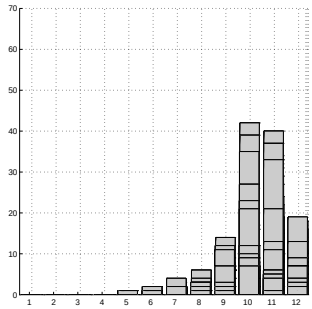

(e) n=1500

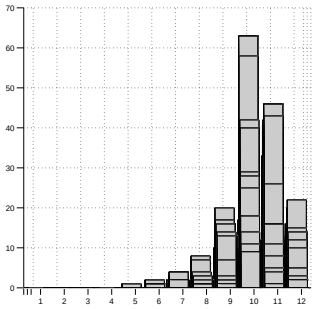

(f) n=2500

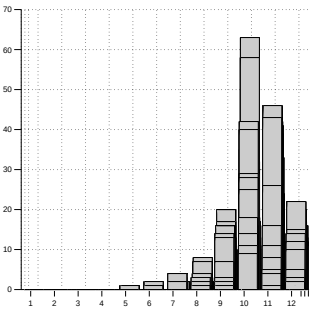

(g) n=4000

Figure 10: Evolution of an SRSV grid. The graphs show a view along the length of a corridor. A wall is located within horizontal bin 10

are worn by personnel at heights consistent with the characteristic standing and sitting heights of those people. Non-vertical surfaces, such as tables, are consequently below the usual height of the Bat, and it is unlikely that a signal from the Bat will reflect from them and reach the receivers.

Use of the method to find only vertical surfaces with Bat system data does not imply any limitation of its use with other positioning systems. For example, signals in proposed UWB positioning systems would be expected to reflect extensively from surfaces of all orientations within the environment.

7 Conclusions and Further Work

We have presented a novel method for surface discovery using reflections. Our results indicate that it can potentially provide a rich source of world information. Our implementation has centred around wall detection, which we have demonstrated with good results based on a relatively small data set. The method in general, however, is easily extended to search for non-vertical reflecting surfaces, by using intersection of prolate spheroids and SRSV cells which record intersection normals in three dimensions.

We envisage this data source being combined with other sources (many of which are discarded by today's positioning systems) to provide robust information about the environment. In particular, we hope to use these, and related, techniques to determine the position and orientation of large flat-screen displays - a common source of problems for ultrasonic positioning which we intend to compensate for. Furthermore, the usage of archived personnel positions can be used to derive complementary environmental information, such as region connectivity and the position of large scale objects [9].

Whilst the results presented here are for an ultrasound-based system, the theory applies equally to any system that can resolve multi-pathed effects. In particular, the methods presented here should transfer directly to Ultra-Wideband (UWB) radio positioning systems, which have the intrinsic capability of resolving and timing multipathed signals [7].

Beyond the niche of pervasive computing, the method can be applied to autonomous navigation and map building. In these fields, we typically use a variety of ranging and signal bouncing techniques to permit a robot to 'learn' its environment using probabilistic methods [15]. SRSV here could provide a useful extra information source that improves the probability calculations. Furthermore, such a robot can be programmed to adopt a motion pattern that targeted specific areas of uncertainty within an environment.

8 Acknowledgements

The authors are grateful to both the EPSRC and AT&T for supporting this work through a research grant and CASE award respectively.

References

[1] M. Addlesee, R. Curwen, S. Hodges, J. Newman, P. Steggles, A. Ward, and A. Hopper. Implementing a sentient computing system. *IEEE Computer*, 34(8), August 2001.

[2] P. Bahl and V. N. Padmanabhan. RADAR: An in-building RF-based user location and tracking system. In *INFOCOM 2*, pages 775–774, 2000.

[3] P. Bahl, V. N. Padmanabhan, and A. Balachandran. Enhancements to the RADAR user location and tracking system. Technical report, Microsoft Research, February 2000.

[4] B. Barshan. Ultrasonic surface profile determination by spatial voting. In *Proceedings of the IEEE Instrumentation and Measurement Technology Conference, Budapest, Hungary*, pages 583–588, May 2001.

[5] B. Barshan and D. Baskent. Comparison of two methods of surface profile extraction from multiple ultrasonic range measurements. *Meas. Sci. Technology*, 11:833–844, April 2000.

[6] D. Bohn. Environmental effects on the speed of sound. *Journal of the Audio Engineering Society*, 36(4):223–231, April 1988.

[7] Time Domain. PulsOn technology overview. Technical report, Time Domain Corporation, 2001. http://www.timedomain.com.

[8] R. O. Duda and P. E. Hart. Use of the hough transform to detect lines and curves in pictures. *Communications of the ACM*, 15(1):11–15, 1972.

[9] R.K. Harle and A. Hopper. Using Personnel Movements For Indoor Autonomous Environment Discovery. To appear in PerCom 2003, 2003.

[10] J. Hightower and G. Borriello. Location sensing techniques. *IEEE Computer*, August 2001.

[11] R. M. Murray, Z. Li, and S. S. Sastroy. *A Mathematical Introduction to Robotic Manipulation*. CRC Press, 1994.

[12] N. B. Priyantha and A. Chakraborty and H. Balakrishnan. The Cricket Location-Support System. *Proceedings of the Sixth Annual ACM International Conference on Mobile Computing Networking*, August 2000.

[13] W. H. Press, S. A. Teukolsky, W. T. Vetterling, and B. P. Flannery. *Numerical Recipes in C*. CUP, 1992.

[14] N. B. Priyantha, K. L. M. Allen, H. Balakrishnan, and S. J. Teller. The cricket compass for context-aware mobile applications. In *Mobile Computing and Networking*, pages 1–14, 2001.

[15] S. Thrun. Learning maps for indoor mobile robot navigation. *Artificial Intelligence*, 99(1):21–71, 1998.

[16] A. M. R. Ward. *Sensor-driven Computing*. PhD thesis, Cambridge University, August 1998.